Clays and Clay Minerals, Vol. 27, No. 5, pp. 327–338, 1979.

ROLE OF IRON REDUCTION IN THE CONVERSION OF SMECTITE TO ILLITE IN BENTONITES IN THE DISTURBED BELT, MONTANA

ERIC ESLINGER,[1] PATRICK HIGHSMITH,[2] DOYLE ALBERS,[3] AND BENJAMIN DEMAYO[4]

Abstract—Cretaceous bentonites were collected in outcrop from the Sweetgrass Arch and the Disturbed Belt in Montana. The mixed-layer illite-smectite (I/S) components of the bentonites from the Sweetgrass Arch have from 0 to 25% illite layers and no detectable structural Fe^{2+}, whereas the samples from the Disturbed Belt have from about 25 to 90% illite layers, and all contain Fe^{2+}. A positive correlation ($r = 0.89$) exists between the percentage of structural iron that is Fe^{2+} and the amount of fixed interlayer K in the I/S.

The higher percentage of illite layers in the samples from the Disturbed Belt is attributed to reactions related to elevated temperatures caused by burial beneath thrust sheets. The increase in Fe^{2+}/Fe^{3+} with increasing percentages of illite layers is tentatively attributed to a redox reaction involving the oxidation of organic matter. Although there is no statistical evidence for an increase in octahedral charge with an increase in illite layers when all the samples are considered together, iron reduction may have contributed as much as 10 to 30% of the increase in total structural charge that occurred in any given sample during metamorphism. The remaining structural charge increase can be attributed to the substitution of Al^{3+} for Si^{4+} in the tetrahedral sites.

Key Words—Bentonite, Illite, Iron reduction, Mixed layer, Montana, Smectite.

INTRODUCTION

The conversion of mixed-layer illite/smectite (I/S) from a structure containing a low percentage of illite layers into a structure containing a high percentage of illite layers during burial metamorphism has been documented by Denoyer de Segonzac (1964), Perry and Hower (1970), Weaver (1960), Weaver and Beck (1971), and Hower *et al.* (1976). This conversion takes place between 50° and 200°C over a depth range of thousands of meters in thick sedimentary sequences. The study of Hower *et al.* (1976) of cuttings from a Gulf Coast well shows that the conversion can be approximated by the isochemical reaction: Smectite + K^+ + Al^{3+}→Illite + Si^{4+}. The K^+ and Al^{3+} for this reaction are apparently derived from the destruction of detrital K-feldspar and micas with at least some of the released Si^{4+} going to form diagenetic quartz.

The fixation of K^+ in the interlayers of I/S is related to an increased negative charge within the clay structure. In Gulf Coast sediments this charge is related to the substitution of Al^{3+} for Si^{4+} in the tetrahedral sites (Weaver and Beck, 1971; Foscolas and Kodama, 1974; Hower *et al.*, 1976). The reduction of structural Fe^{3+} to Fe^{2+} could also cause an increase in the structural charge, as has been suggested by Perry and Hower (1970), but this mechanism has not been previously demonstrated. Muffler and White (1969) reported increases in FeO/Fe_2O_3 with depth in the Salton Sea geothermal area, but their data are on bulk samples possessing several iron-bearing minerals. Weaver and Beck (1971, p. 52) stated that the data of Shaw (1956) indicate that Fe^{2+}/Fe^{3+} values increase during low-grade metamorphism. However, Shaw's data are on bulk analyses and compare shales plus slates, schists and gneisses. Weaver and Beck (1971, Table 7) listed FeO and Fe_2O_3 values for seven bulk samples collected from a Gulf Coast well. Even though the samples had been treated prior to analysis to remove free iron oxides, they still contained variable amounts of illite, chlorite, a mixed-layered phase, and siderite, all of which contain iron. Therefore, although the authors hinted at an increase in FeO/Fe_2O_3 with depth, it is not surprising that such a trend is ill defined. In none of the above studies were changes in FeO/Fe_2O_3 within a single phase monitored.

The purpose of this study was to investigate with Mössbauer spectroscopy the valence state of iron in I/S from a metamorphic sequence to see if a correlation exists between Fe^{2+}/Fe^{3+} and the percentage of illite layers. Samples used were <0.1 μm (equivalent spherical diameter) size fractions of Cretaceous bentonites collected in outcrop from the Sweetgrass Arch and the Disturbed Belt, Montana. Figure 1 shows the location of the sample sites, and Tables 1 and 2 give pertinent stratigraphic data. The bentonites from the Sweetgrass Arch are predominantly I/S with 0–25% illite layers. The bentonites from the Disturbed Belt are predomi-

[1] Department of Geology, West Georgia College, Carrollton, Georgia 30118.
[2] Department of Geophysical Sciences, Georgia Institute of Technology, Atlanta, Georgia 30303.
[3] Department of Geology, University of Idaho, Moscow, Idaho 83843.
[4] Department of Physics, West Georgia College, Carrollton, Georgia 30118.

nantly I/S with 25–90% illite layers. The <0.1-μm size fraction of most of these bentonites is essentially 100% I/S; sample LTE-23 contains a trace of kaolinite or chlorite.

A K/Ar study of both bentonites and shales from this region (Hoffman *et al.*, 1976) combined with field studies (Mudge, 1970, 1972a, 1972b) and theoretical heat-flow studies (Oxburgh and Turcotte, 1974) strongly suggests that the temperatures that promoted the conversion of smectite into illite in this area were not the result of simple geosynclinal burial as in the Gulf Coast. Elevated temperatures were due to the accumulation of heat beneath stacked thrust sheets. Hoffman and Hower (1979) documented on a larger scale the mineralogical and chemical variations in bentonites and shales of this region.

ANALYTICAL PROCEDURES

Sample preparation

The bentonite samples were dispersed with an ultrasonic generator in a buffer solution of sodium acetate (Jackson, 1956), heated with intermittent stirring at about 80°C for 30 min, and then washed several times by centrifuging in fresh buffer until the supernatant was clear. The samples were then boiled in Ni dishes for 5 min in 2% Na_2CO_3 and centrifuged until flocculation occurred. The supernatant was decanted, and the flocculant was repeatedly centrifuged in distilled water until flocculation ceased. These treatments promote dispersion by dissolving amorphous materials. Size separations at 1.0 μm and 0.1 μm were made using centrifugation techniques.

X-ray powder diffraction

Slides for X-ray powder diffraction (XRD) of the <0.1-μm fraction were made by allowing aqueous suspensions of the samples to evaporate on glass slides to produce oriented mounts. These slides were then solvated with ethylene glycol and X-rayed at 2° 2θ/min from 33° to 2° 2θ with a Norelco XRD-5 diffractometer equipped with a single-crystal monochrometer and using CuKα radiation. Additional XRD scans at ⅛° 2θ/min were made to determine the average percentage of illite layers using the technique of Reynolds and Hower (1970). The precision of this determination is about ±5% illite layers.

Chemical analyses

Chemical analyses of the <0.1-μm fraction were made by atomic absorption spectroscopy using the technique of Medlin *et al.* (1969). Replicate analyses of three of the samples indicated that the precision (average error) of the elemental concentrations was almost always less than 0.2%. Reproducibility data for one of these samples (LT-21) are given in Table 3. Total water in several of the samples was determined using weight loss by placing a separate aliquot of each sample in a desiccator for several days and then heating a weighed amount of each sample in a platinum crucible at 1000°C for 30 min.

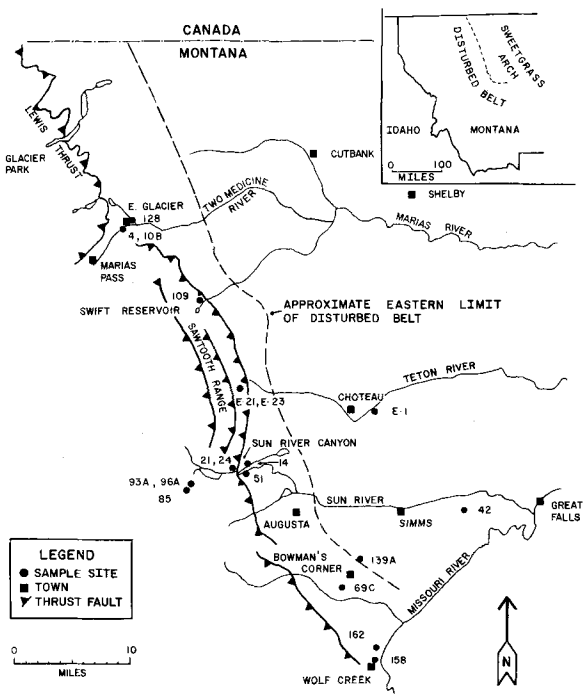

Figure 1. Disturbed Belt of Montana showing location of sample sites.

Table 1. Location, stratigraphic unit, and thickness of bentonite beds.

Sample	Location[1]	Stratigraphic unit	Thickness (cm)
LT-1	S.A.	Taft Hill	3
LT-4	D.B.	Kevin Shale	15
LT-10B	D.B.	Kevin Shale	8
LT-14	D.B.	Kevin Shale	25
LT-21	D.B.	Vaughn	5
LT-24	D.B.	Vaughn	8
LT-42	S.A.	Cone Calcareous	91
LT-51	D.B.	Kevin Shale	23
LT-69C	D.B.	Two Medicine	31
LT-85	D.B.	Cone Calcareous	213
LT-93A	D.B.	Kevin Shale	31
LT-96A	D.B.	Kevin Shale	31
LT-109	D.B.	Upper Cretaceous	31
LT-128	D.B.	Kevin Shale	31
LT-139A	S.A.	Two Medicine	152
LT-158	D.B.	Telegraph Creek	4
LT-162	D.B.	Kevin Shale	5
LTE-1	S.A.	Colorado	13
LTE-21	D.B.	Colorado	5
LTE-23	D.B.	Colorado	13

[1] S.A. = Sweetgrass Arch; D.B. = Disturbed Belt.

Table 2. Stratigraphy in the Disturbed Belt–Sweetgrass Arch area (after Mudge, 1972a).

Series	Group	Formation	Member
UPPER CRETACEOUS	Montana	Two Medicine Virgelle Sandstone Telegraph Creek	
	Colorado	Marias River Shale	Kevin Shale Ferdig Shale Cone Calcareous Floweree Shale
LOWER CRETACEOUS		Blackleaf	Vaughn Taft Hill Flood Shale
		Kootenai	

Mössbauer spectroscopy

Mössbauer spectroscopy scans of approximately 200 mg of the <0.1-μm fraction of the samples were made using a conventional acceleration Mössbauer spectrometer having a Co^{57} source imbedded in Pa. Each sample was bombarded for three days at room temperature, and the resultant spectra were fitted by least squares to Lorentzian-shaped lines using a computer program. The Fe^{2+}/Fe^{3+} ratios were determined from peak-area ratios taken from the spectra. The oxidation state of the iron was determined by comparison with data listed by Bowen *et al.* (1968) and Weaver *et al.* (1967) who showed for a variety of three-layer phyllosilicates that the isomer shift (I.S.) of Fe^{2+} is between 1.0 and 1.3 mm/sec (relative to enriched iron foil), that the I.S. of Fe^{3+} is between 0.2 and 0.6 mm/sec, that the quadrupole splitting (Q.S.) of Fe^{2+} is between 2.2 and 3.0 mm/sec, and that the Q.S. of Fe^{3+} is between 0.5 and 1.1 mm/sec. Although the "right hand" peak of the Fe^{2+} doublet is superimposed on the "right hand" peak of the Fe^{3+} doublet, the computer is programmed to resolve these two peaks. Since the intensities of such calculated "right hand" Fe^{2+} peaks commonly differed by a factor of two or more from the intensities of the "left hand" Fe^{2+} peaks, the "left hand" peak intensities for Fe^{2+} were multiplied by two in order to determine total area intensities for Fe^{2+}. Thus, the "right hand" Fe^{2+} peak intensities were not used in the calculations.

Structural formulae

Structural formulae for the I/S were calculated by normalizing cation analyses to a theoretical structure containing $O_{10}(OH)_2$ with a negative charge of 22. The problems in determining a formula in this manner for I/S for which the structural details are not known have been discussed by Hower and Mowatt (1966). Preignition structural FeO and Fe_2O_3 were calculated from total iron (as Fe_2O_3) obtained from atomic absorption and from the Fe^{2+}/Fe^{3+} ratios obtained from Mössbauer spectroscopy. All Fe^{2+} and Fe^{3+} was assumed to be in the octahedral sites. The cation-exchange capacity (CEC) was estimated using the linear relationship between CEC and percent illite layers [CEC = 89 − (0.8) (% illite layers)] determined by Hower and Mowatt (1966). Since the sample preparation involved repeated washings with sodium acetate, the samples were effectively Na-saturated. Therefore, all of the potassium as well as all of the magnesium was assumed to be "fixed." All of the sodium and calcium was assumed to be exchangeable. Titanium was included in the structural formula on the basis of a report (Dolcater *et al.*, 1970) that more than half of the Ti in two bentonites was structural and not in a separate phase. Manganese was not included in the structural formulae because the MnO_2 concentrations were insignificant.

The assumption that all of the iron is located in the octahedral sites is probably good. Although Mössbauer spectroscopy of nontronites (Bischoff, 1972; Goodman *et al.*, 1976; Weaver *et al.*, 1967) and glauconites (Taylor *et al.*, 1968) and acid dissolution of nontronites (Osthaus, 1954) showed that Fe^{3+} can exist in the tetrahedral sites of these iron-rich analogues of I/S, Mössbauer studies of montmorillonites (Rozenson and Heller-Kallai, 1976c; Malathi *et al.*, 1969; Weaver *et al.*, 1967) indicate no iron in the tetrahedral sites.

RESULTS AND DISCUSSION

Chemical analyses are given in Table 3 and Mössbauer spectroscopy data are given in Table 4. XRD patterns and Mössbauer spectra of four representative samples are shown in Figures 2 and 3. The I.S., Q.S., and single doublet of the spectra of sample LT-42 (Figure 4A) indicate that only Fe^{3+} is present. The other three spectra shown in Figure 3 are of samples that contain both Fe^{3+} and Fe^{2+}. The structural formulae and

Table 3. Chemical analyses of bentonites[1] (weight %).

	LT-42	LT-139A	LT-1	LT-69C	LT-158	LT-4	LT-128	LT-85
SiO_2	55.1	47.8	44.5	46.5	54.5	46.5	53.2	49.0
TiO_2	0.32	0.185	0.19	0.23	0.23	0.185	0.19	0.00
Al_2O_3	19.36	20.46	20.3	22.83	23.82	25.60	26.36	24.1
Fe_2O_3	1.35	3.95	4.95	2.35	2.15	1.01	1.38	1.45
FeO	0.00	0.00	0.00	0.24	0.39	0.30	0.37	0.27
MgO	3.86	1.64	1.58	1.60	2.20	1.64	1.84	2.13
K_2O	0.55	0.62	0.95	1.95	2.57	3.25	3.93	4.00
MnO	0.016	0.021	0.03	0.02	0.021	0.018	0.016	0.021
CaO	0.71	0.71	0.95	0.74	0.71	0.75	0.72	0.18
Na_2O	2.85	3.92	7.05	4.10	0.21	2.32	0.90	3.59
TOTAL	84.1	79.3	80.5	80.6	86.8	81.6	88.9	84.74
L.O.I.[2]	17.53	20.41	—	22.77	14.43	17.48	13.26	—
TOTAL	101.6	99.7	—	103.4	101.2	99.1	102.2	—

	LT-96A	LT-93A	LT-162	LT-51	LT-10B	LT-21[3]	D%	LT-21[4]	D%	LT-109	LT-24	LTE-21	LTE-23
SiO_2	51.7	50.6	51.0	48.5	48.0	46.8	1.0	44.5	0.0	51.8	51.0	50.5	46.3
TiO_2	0.19	0.190	0.15	0.10	0.005	0.275	0.0	0.16	0.02	0.10	0.08	0.23	0.00
Al_2O_3	24.3	24.00	28.2	27.9	27.2	25.20	0.0	25.6	0.37	23.64	26.9	27.50	28.8
Fe_2O_3	1.83	1.29	1.29	0.95	1.20	2.72	0.02	2.82	0.02	2.34	2.53	1.54	2.59
FeO	0.36	0.55	0.20	0.65	0.13	0.82	0.02	0.84	0.02	0.59	0.89	0.75	1.09
MgO	2.62	2.44	1.77	1.42	1.58	1.62	0.01	1.50	0.01	3.08	1.51	1.84	2.00
K_2O	4.50	4.55	4.70	4.71	4.40	4.90	0.01	5.12	0.02	5.10	5.61	5.70	5.35
MnO	0.013	0.018	0.012	0.018	0.018	0.021	0.0	0.022	0.0	0.016	0.021	0.018	0.021
CaO	0.18	0.74	0.21	0.75	0.65	0.84	0.0	0.30	0.0	0.79	0.17	0.71	0.17
Na_2O	0.42	2.00	0.62	1.67	2.82	0.88	0.0	1.12	0.02	1.87	1.23	0.30	0.44
TOTAL	85.9	86.4	88.2	86.7	86.0	84.1		81.9		89.3	89.9	88.9	86.81
L.O.I.[2]	—	13.40	—	15.15	—	16.16		—		10.20	—	10.68	—
TOTAL	—	99.8		101.8	—	100.3	—	—		99.5	—	99.7	

[1] Listed in order of increasing percentage of illite layers.
[2] Loss on ignition (see text).
[3] Analysis by D.A., average error ($\bar{D}$) is for two aliquots.
[4] Analysis by P.H., average error ($\bar{D}$) is for three aliquots.

Table 4. Quadrupole splitting, isomer shift, Fe^{2+}/Fe^{3+}, and $(Fe^{2+}/Fe^{2+} + Fe^{3+}) \times 100\%$.

	Fe^{2+}		Fe^{3+}			
Sample[1]	Quadrupole shift (mm/sec)	Isomer shift (mm/sec)	Quadrupole shift (mm/sec)	Isomer shift (mm/sec)	Fe^{2+}/Fe^{3+}	$(Fe^{2+}/Fe^{2+} + Fe^{3+}) \times 100\%$
LT-42	—	—	0.69	0.36	0.0	0
LT-139A	—	—	0.59	0.35	0.0	0
LTE-1	—	—	1.09	0.37	0.0	0
LT-1	—	—	0.60	0.35	0.0	0
LT-69C	2.73	1.21	0.57	0.33	0.10	9
LT-158	2.90	1.15	0.67	0.36	0.24	19
LT-4[3]	—	—	—	—	0.33	25
LT-128	2.85	1.11	0.73	0.33	0.30	23
LT-85	2.92	1.09	0.82	0.27	0.21	17
LT-96A	2.87	1.14	0.69	0.33	0.31	24
LT-93A	2.89	1.18	0.88	0.35	0.47	32
LT-162	2.89	1.13	0.84	0.27	0.36	27
LT-51	2.83	1.20	0.47	0.43	0.54	35
LT-14[2]	2.87	1.17	0.69	0.34	0.57	36
LT-10B[4]	3.57	1.47	0.65	0.32	0.12	11
LT-21	2.91	1.13	0.60	0.35	0.33	25
LT-109	2.78	1.15	0.56	0.38	0.29	23
LT-24	2.87	1.14	0.69	0.33	0.48	32
LTE-21	2.86	1.14	0.55	0.32	0.53	35
LTE-23	2.85	1.07	0.72	0.31	0.46	32

[1] Listed in order of increasing percentage of illite layers.
[2] Chemical analyses (cf. Table 3) of LTE-1 (15% illite layers) and LT-14 (67% illite layers) were not done.
[3] Resolution of "right-hand" Fe^{2+} peak too poor to determine isomer and quadrupole shifts.
[4] Resolution of "lefthand" Fe^{2+} peak very poor.

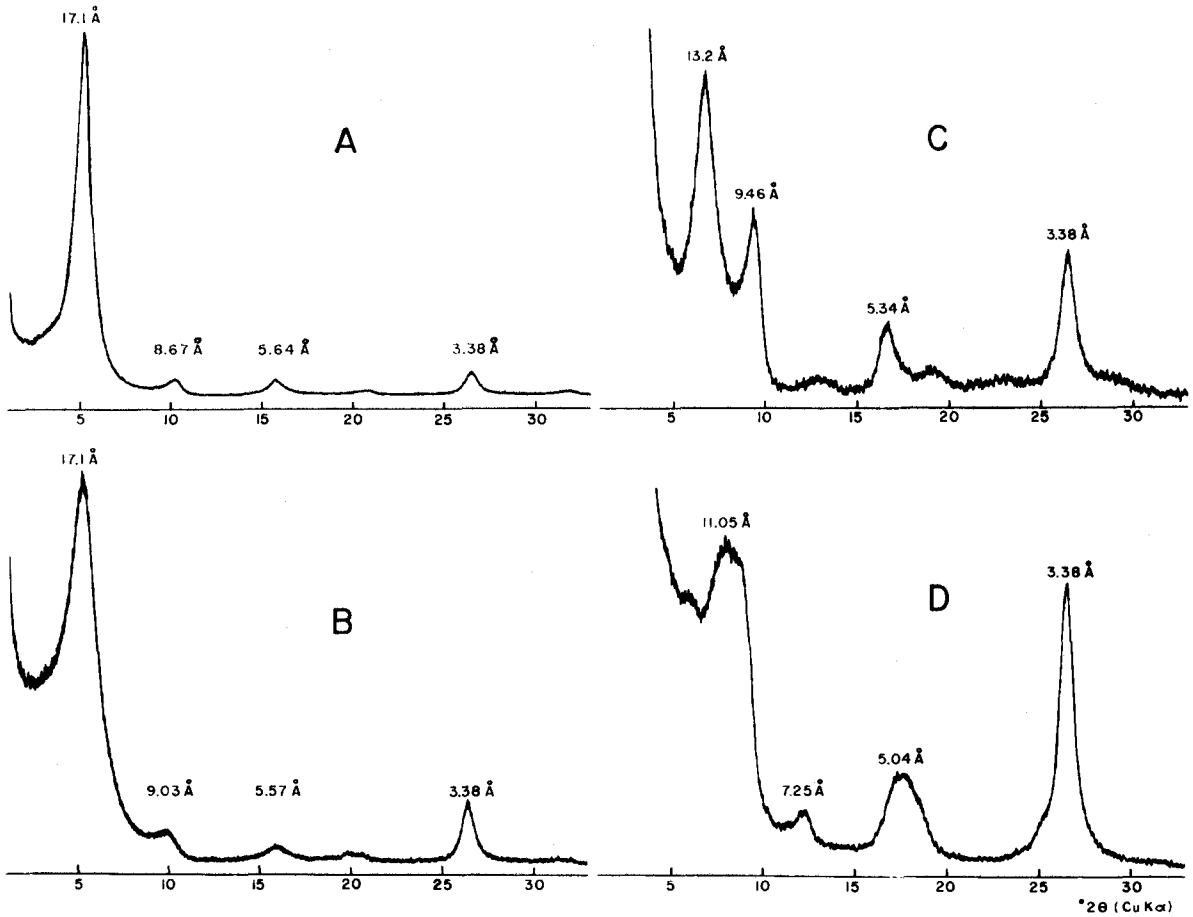

Figure 2. Representative X-ray powder diffraction patterns. (A) LT-42, (B) LT-69C, (C) LT-93A, and (D) LTE-23. Samples were "oriented" and saturated with ethylene glycol. Samples LT-42 (5% illite layers) and LT-69C (28% illite layers) are randomly mixed-layered, sample LT-93A (63% illite layers) is IM ordered mixed-layered, and sample LTE-23 (90% illite layers) is IMII ordered mixed-layered (Reynolds and Hower, 1970). Sample LTE-23 contains some kaolinite or chlorite.

percent illite layers data are given in Table 5. The sum of the cations in the octahedral position is equal to or less than 2.06 per $O_{10}(OH)_2$ for each sample except LTE-23 which has a sum of 2.13. Because this sample contains a trace of kaolinite or chlorite, the apparent excess octahedral occupancy may be due to cations that are actually in kaolinite or chlorite.

Figure 4 shows how K_n, Al_n, and Si_n [where n denotes the number of atoms per $O_{10}(OH)_2$] vary with the percentage of illite layers. The trends indicate that I/S in the Disturbed Belt has undergone a reaction similar to I/S in the Gulf Coast (Hower *et al.*, 1976) as discussed above. Figure 5 shows how K_n increases with the structural charge. The other points on this graph are from the same type of plot for illites and I/S from argillaceous sediments (Hower and Mowatt, 1966). The upper line represents the relationship that would exist between K_n and the structural charge if all the charge were satisfied by fixed K; the ordinate between this line and a line through the points represents the amount of structural charge satisfied by exchangeable interlayer cations. The data from this study complement those in Hower and Mowatt (1966) particularly in the low charge range and allow the extrapolation of the K_n vs. structural charge trend to zero K_n. This trend indicates that "pure" smectite (no illite layers) having no fixed K would have a structural charge of about −0.40 per $O_{10}(OH)_2$, all of which would be satisfied by exchangeable interlayer cations.

It is significant that the four samples from the Sweetgrass Arch have no detectable Fe^{2+} but that all of the samples from the Disturbed Belt do have Fe^{2+} (cf. Table 4). Figure 6 shows that there is a positive correlation ($r = 0.89$) between $Fe^{2+}/(Fe^{2+} + Fe^{3+})$ and K_n. Thus, the data strongly suggest that prior to burial the smectites contained little if any structural Fe^{2+}, but as heating occurred during burial some of the Fe^{3+} was reduced to Fe^{2+}.

Rozenson and Heller-Kallai (1978) demonstrated that structural Fe^{2+} in montmorillonites can be oxidized

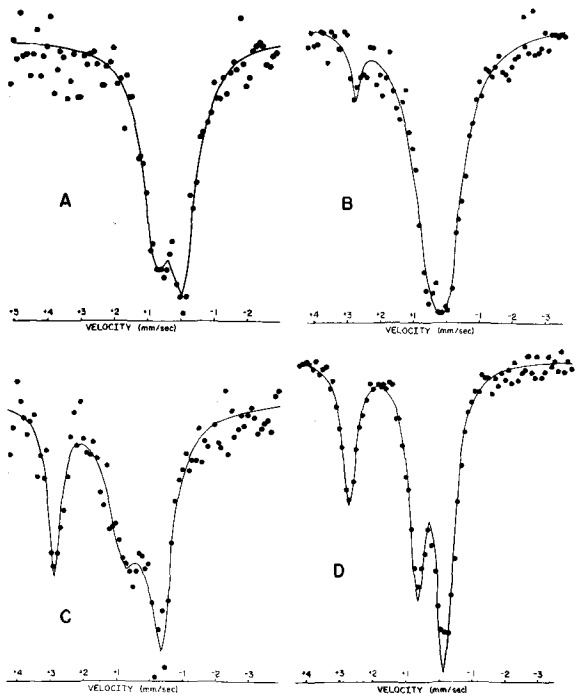

Figure 3. Mössbauer spectra of the samples whose X-ray powder diffraction patterns are shown in Figure 3. (A) LT-42, (B) LT-69C, (C) LT-93A, and (D) LTE-23. The inner doublet (the only doublet present in Figure 3a) is from Fe^{3+}. The outer doublet is from Fe^{2+}; the "right hand" peak of the Fe^{2+} doublet is superimposed onto the "right hand" peak of the Fe^{3+} doublet. Dots are data points and the line delineates the computer-fitted curve.

by mild chemical treatments. Thus, the Fe^{2+}/Fe^{3+} data given in Table 4 perhaps should be considered as minimum values. However, because the correlation of $Fe^{2+}/(Fe^{2+} + Fe^{3+})$ with K_n (cf. Figure 6) is statistically significant, any alteration in oxidation state of iron that might have occurred during laboratory treatment of the samples was apparently not great enough to mask the true nature of the iron in the I/S.

Rozenson and Heller-Kallai (1976a, 1976b) also experimentally reduced Fe^{3+} to Fe^{2+} in montmorillonites. They inferred that local charge balance is maintained within the octahedral layer by the protonation of hydroxyl groups and that the required protons are derived from water released from the interlayers. Furthermore, they demonstrated that the reaction is reversible if the montmorillonite is reoxidized. Accordingly, an increase in Fe^{2+}/Fe^{3+} with K_n would be expected since interlayer water is released as smectite layers collapse. However, an intuitive argument can be made that the correlation of $Fe^{2+}/(Fe^{2+} + Fe^{3+})$ with K_n (cf. Figure 6) would probably not exist in these samples if the octahedral charge were locally balanced by protonation because the protonation reaction *is* readily reversible in an oxidizing environment as demonstrated by Rozenson and Heller-Kallai (1976a), and, all of the bentonites were in an oxidizing "outcrop" environment for some years.

If protonation of hydroxyls has not occurred in the bentonites, the reduction of Fe^{3+} to Fe^{2+} would tend to cause an increase in the octahedral charge. The appar-

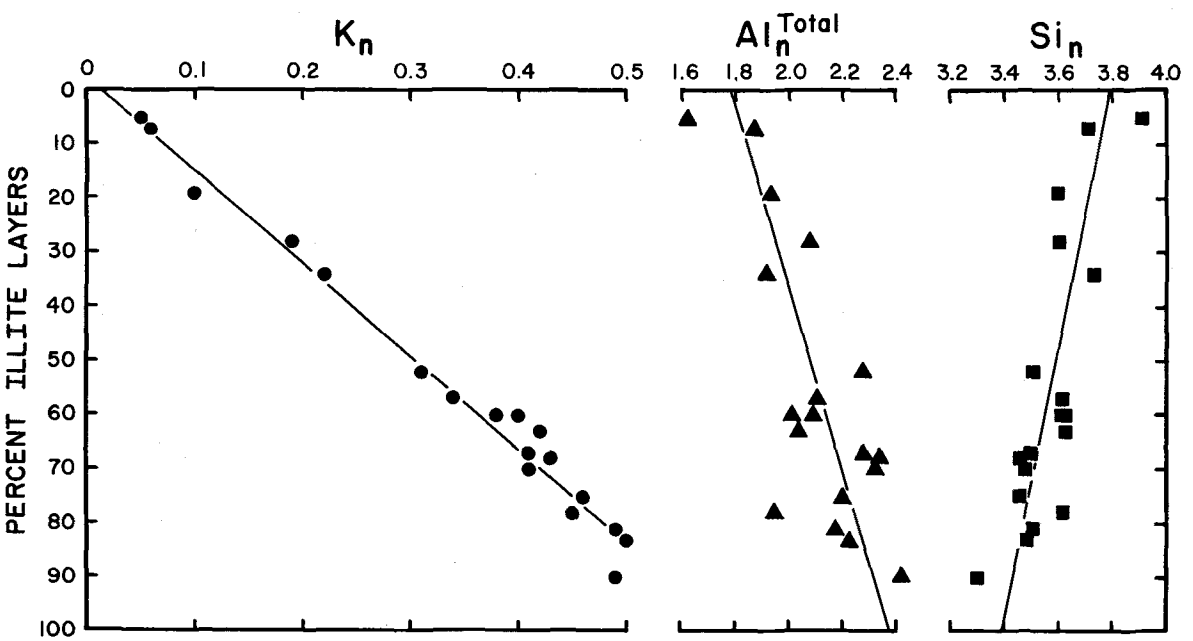

Figure 4. Variation of K_n (fixed), Al_n, and Si_n [per $O_{10}(OH)_2$] with percentage of illite layers. K_n, r = 0.99; Al_n, r = 0.76; Si_n, r = 0.78.

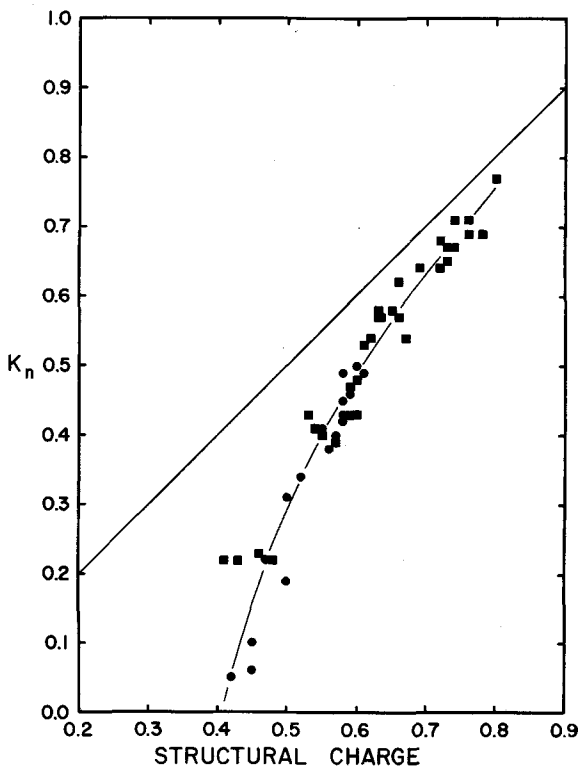

Figure 5. K_n ["fixed" potassium per $O_{10}(OH)_2$] vs. total structural charge. Data points: ● this paper; ■ Hower and Mowatt (1966).

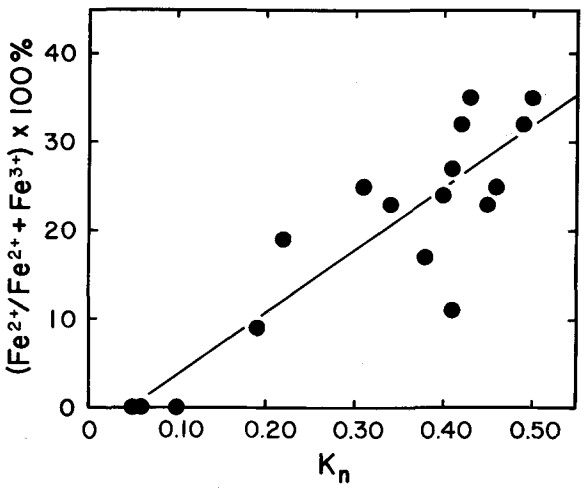

Figure 6. Ratio of $Fe^{2+}/(Fe^{2+} + Fe^{3+}) \times 100\%$ vs. K_n [fixed K per $O_{10}(OH)_2$], r = 0.89.

ent effect of iron reduction, without concomitant protonation, on the total structural charge was estimated by making the following assumptions: (1) The total structural charge of each of the I/S samples was 0.40 per $O_{10}(OH)_2$ before the sample was metamorphosed. The value of 0.40 comes from Figure 5 and undoubtedly represents an average charge for I/S having no fixed K; the original charge of a given I/S might reasonably have been 0.40 ± 0.05 per $O_{10}(OH)_2$. (2) All iron in each of the I/S was Fe^{3+} before metamorphism. This cannot be proven but seems to be a reasonable assumption since none of the samples from the Sweetgrass Arch contains Fe^{2+}. (3) Total Fe, Mg^{2+}, and Ti^{4+} are immobile. Again, this assumption cannot be proven but is made because there is no correlation of any of these ions with percent illite layers (cf. Table 5). Thus, variations in these values between samples are attributed to premetamorphic differences. The results of the calculations are given in Table 6. Most of the values range between 10 and 30%, giving the impression that iron reduction can contribute significantly to the total increase in charge on the structure. However, it can be argued that most of the increase in structural charge is due to an increase in the tetrahedral charge.

Figure 7 shows how octahedral and tetrahedral charge varies with percent illite layers. The apparent correlation of decreasing octahedral charge with percent illite layers (r = 0.50) is probably not significant since elimination of samples LTE-23 and LT-42 from the data set drastically lowers the correlation coefficient (to r = 0.14). It is significant that there is no statistical evidence of an increase in octahedral charge with percent illite layers. However, there is a significant correlation (r = 0.78 using samples LTE-23 and LT-42; r = 0.65 if those samples are not used) of tetrahedral charge with percent illite layers that is a direct function of the amount of substitution of Al for Si in the tetrahedral layers. This substitution is analagous to that occurring in modern Gulf Coast sediments (Hower *et al.*, 1976) as was discussed in the introduction of this paper. The effect of iron reduction on the increase in structural charge is apparently minimal possibly due to the small amount of total iron in these samples. Using an average value of 20% as the increase in structural charge due to iron reduction (cf. Table 6), an increase in structure charge from −0.40 to −0.60 (cf. Figure 5) would mean an increase in octahedral charge of only (0.20) × (−0.20) = (−0.04). Though such an increase may have occurred for a given sample, the scatter in the data precludes the conclusion that this has happened for all of the samples, and thus a significant effect on the octahedral charge due to iron reduction cannot be construed for all of the samples.

The changes in charge distribution that accompanied metamorphism can be generalized (Table 7) as follows: As the percentage of illite layers in I/S increases from 0 to 90 the tetrahedral charge increases from −0.30 to −0.50 while the octahedral charge of about −0.10 does not change in a systematic manner (cf. Figure 7). Thus, the total structure charge increases from about −0.40 to about −0.60. This layer charge is balanced by an interlayer charge comprised of exchangeable cations

Table 5. Chemical formulae [cations per $O_{10}(OH_2)$] and percentage of illite layers.

Positions	Ion	LT-42	LT-139A	LT-1	LT-69C	LT-158	LT-4	LT-128	LT-85	LT-96A	LT-93A	LT-162
	Si	3.91	3.71	3.60	3.60	3.73	3.51	3.62	3.61	3.63	3.63	3.50
Tetrahedral	Al	0.09	0.29	0.40	0.40	0.27	0.49	0.38	0.39	0.37	0.37	0.50
	Charge	−0.09	−0.29	−0.40	−0.40	−0.27	−0.49	−0.38	−0.39	−0.37	−0.37	−0.50
	Al	1.53	1.58	1.54	1.68	1.65	1.79	1.73	1.70	1.64	1.67	1.78
	Fe^{3+}	0.07	0.23	0.30	0.14	0.11	0.06	0.07	0.08	0.10	0.07	0.06
	Fe^{2+}	0.00	0.00	0.00	0.02	0.02	0.02	0.02	0.02	0.02	0.03	0.02
Octahedral	Ti	0.02	0.01	0.01	0.01	0.01	0.01	0.01	0.00	0.00	0.01	0.01
	Mg	0.41	0.19	0.19	0.18	0.22	0.18	0.19	0.23	0.27	0.26	0.18
	Sum	2.02	2.01	2.04	2.03	2.01	2.06	2.02	2.03	2.03	2.03	2.05
	Charge	−0.33	−0.16	−0.06	−0.10	−0.20	−0.01	−0.14	−0.17	−0.20	−0.21	−0.04
	Total lattice charge	−0.42	−0.45	−0.46	−0.50	−0.47	−0.50	−0.52	−0.56	−0.57	−0.58	−0.54
	K	0.05	0.06	0.10	0.19	0.22	0.31	0.34	0.38	0.40	0.42	0.41
	CEC[1]	0.37	0.39	0.35	0.32	0.25	0.22	0.18	0.18	0.17	0.17	0.14
Interlayer	Interlayer charge	+0.42	+0.45	+0.45	+0.51	+0.47	+0.53	+0.52	+0.56	+0.57	+0.59	+0.55
% Illite layers[2]		5	7	19	28	34	52	57	60	60	63	67

Position	Ion	LT-51	LT-10B	LT-21	LT-109	LT-24	LTE-21	LTE-23
	Si	3.46	3.48	3.46	3.62	2.51	3.49	3.30
Tetrahedral	Al	0.54	0.52	0.54	0.38	0.49	0.51	0.70
	Charge	−0.54	−0.52	−0.54	−0.38	−0.49	−0.51	−0.70
	Al	1.80	1.80	1.66	1.57	1.69	1.72	1.72
	Fe^{3+}	0.05	0.07	0.15	0.12	0.13	0.08	0.14
	Fe^{2+}	0.04	0.01	0.05	0.03	0.05	0.04	0.06
Octahedral	Ti	0.01	0.00	0.02	0.01	0.00	0.01	0.00
	Mg	0.15	0.17	0.18	0.32	0.16	0.19	0.21
	Sum	2.05	2.05	2.05	2.05	2.03	2.05	2.13
	Charge	−0.03	−0.03	−0.05	−0.19	−0.12	−0.08	+0.12
	Total lattice charge	−0.58	−0.55	−0.59	−0.57	−0.61	−0.60	−0.58
	K[1]	0.43	0.41	0.46	0.45	0.49	0.50	0.49
	CEC[1]	0.15	0.14	0.13	0.11	0.10	0.10	0.07
Interlayer	Interlayer charge	+0.58	+0.55	+0.59	+0.56	+0.59	+0.60	+0.56
% Illite layers[2]		68	70	75	78	81	83	90

[1] Estimated from % illite layers (see text); meq/100 g.
[2] The first five samples tabulated are randomly interstratified I/S; the others are ordered (Reynolds and Hower, 1970).

whose charge contribution decreases from +0.40 to +0.10 and fixed cations (K) whose charge contribution increases from 0.0 to +0.50 (cf. Figure 5 and Table 5). Thus, the total interlayer charge increases from about +0.40 to about +0.60.

Although the mechanism that may cause iron reduction is unknown, one possibility is that the reduction of iron is a half-reaction for which the oxidation of organic matter trapped in the sediments is the complementary half-reaction. The relative amounts of charge increase due to iron reduction versus tetrahedral substitution of Al for Si would be affected not only by the presence of oxidizable organic matter but also by the ease of substitution of Al for Si. It follows that Fe reduction might become more important in those samples having high percentages of illite layers since access of Al to a tetrahedral site would be more difficult once the adjacent interlayer space has collapsed. Although there is some indication of this trend from the data in Table 6 the data are too few and scatter in the data is too great to suggest that the data actually fit the above model.

Hoffman and Hower (1979) estimated the maximum burial temperature of those samples having fewer than about 25% illite layers to have been about 60°C. Since those samples having fewer than about 25% illite layers contain no Fe^{2+}, the reduction of iron would have been

Table 6. Apparent percentage of structural charge increase due to iron reduction.

Sample[1]	Lattice charge	Fe_n^{2+}	% Due to iron reduction[2]
LT-42	0.42	0.00	0
LT-139A	0.45	0.00	0
LT-1	0.46	0.00	0
LT-69C	0.50	0.02	20
LT-158	0.47	0.02	29
LT-4	0.50	0.02	20
LT-128	0.52	0.02	17
LT-85	0.56	0.02	13
LT-96A	0.57	0.02	12
LT-93A	0.58	0.03	17
LT-162	0.54	0.02	14
LT-51	0.58	0.05	28
LT-10B	0.55	0.01	7
LT-21	0.59	0.05	26
LT-109	0.57	0.03	18
LT-24	0.61	0.05	24
LTE-23	0.58	0.06	33

[1] Samples are listed in order of increasing percentage of illite layers.

[2] $[Fe_n^{2+}/(\text{structure charge} - 0.40)] \times 100\%$.

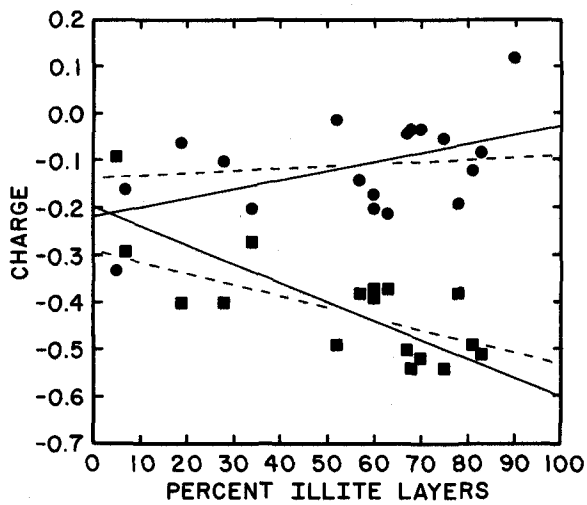

Figure 7. ●, octahedral charge vs. percent illite layers. Solid line: all data used (r = 0.50); dashed line: samples LT-42 and LTE-23 not used (r = 0.14). ■, tetrahedral charge vs. percent illite layers. Solid line: all data used (r = 0.78); dashed line: samples LT-42 and LTE-23 not used (r = 0.65).

initiated at burial temperatures of about 60°C. Hoffman and Hower (1979) estimated the burial temperatures of those samples with greater than about 25% illite layers to have been between 100° and 200°C.

The only other data in the literature that give both structural formulae and Fe^{2+}/Fe^{3+} determined by the same workers in a suite of I/S samples are those of Hower and Mowatt (1966). Figure 8 shows how $Fe^{2+}/(Fe^{2+} + Fe^{3+})$ in the I/S varies with K_n. There is a rough trend of increasing percentage of Fe^{2+} with K_n if the two samples of Cenozoic age (Wilcox Nos. 1 and 2) are ignored. Values of samples from the Disturbed Belt (cf. Figure 6) plot between the two dashed lines. Also shown in Figure 8 are the average percentages of Fe^{2+} (of total iron), the K_n values of 101 montmorillonites and beidellites (Weaver and Pollard, 1973, p. 56), and 15 illites (Weaver and Pollard, 1973, p. 11). The average percentage of Fe^{2+} in the illites is greater than that in the montmorillonites and beidellites. This is the trend that would be expected if most illites form from the metamorphism of montmorillonite-beidellites and if iron reduction generally occurs during that metamorphism.

Table 7. Location and magnitude of structural and interlayer charge in illite/smectites.

			Percent illite layers	
			0	90
Charge	Structural	Tetrahedral	−0.30	−0.50
		Octahedral	−0.10	−0.10
		TOTAL	−0.40	−0.60
	Interlayer	Exchangeable	+0.40	+0.10
		Fixed	+0.00	+0.50
		TOTAL	+0.40	+0.60

CONCLUSIONS

1. None of the samples from the Sweetgrass Arch, but all of the samples from the Disturbed Belt, contain detectable structural Fe^{2+}.

2. There is a positive correlation (r = 0.89) between the percentage of iron that is Fe^{2+} and K_n in the I/S component of the bentonites.

3. The lack of a statistical correlation between octahedral charge and percent illite layers precludes the conclusion that iron reduction plays a major role in increasing the structural charge in all of the samples. However, the contribution of iron reduction to the increase in total structural charge that has occurred in individual samples during metamorphism can be estimated to be between 10 and 30% if it is assumed that all of the iron was originally Fe^{3+}, that the original structural charge was −0.40 per $O_{10}(OH)_2$, that octahedral cations are immobile, and that octahedral charge balance is not maintained by protonation.

4. Although the data neither prove nor disprove that protonation has occurred, the reversible nature of a protonation reaction does not lend itself to an explanation of the correlation of Fe^{2+}/Fe^{3+} with percent illite layers.

5. The reduction of iron is possibly a redox half-re-

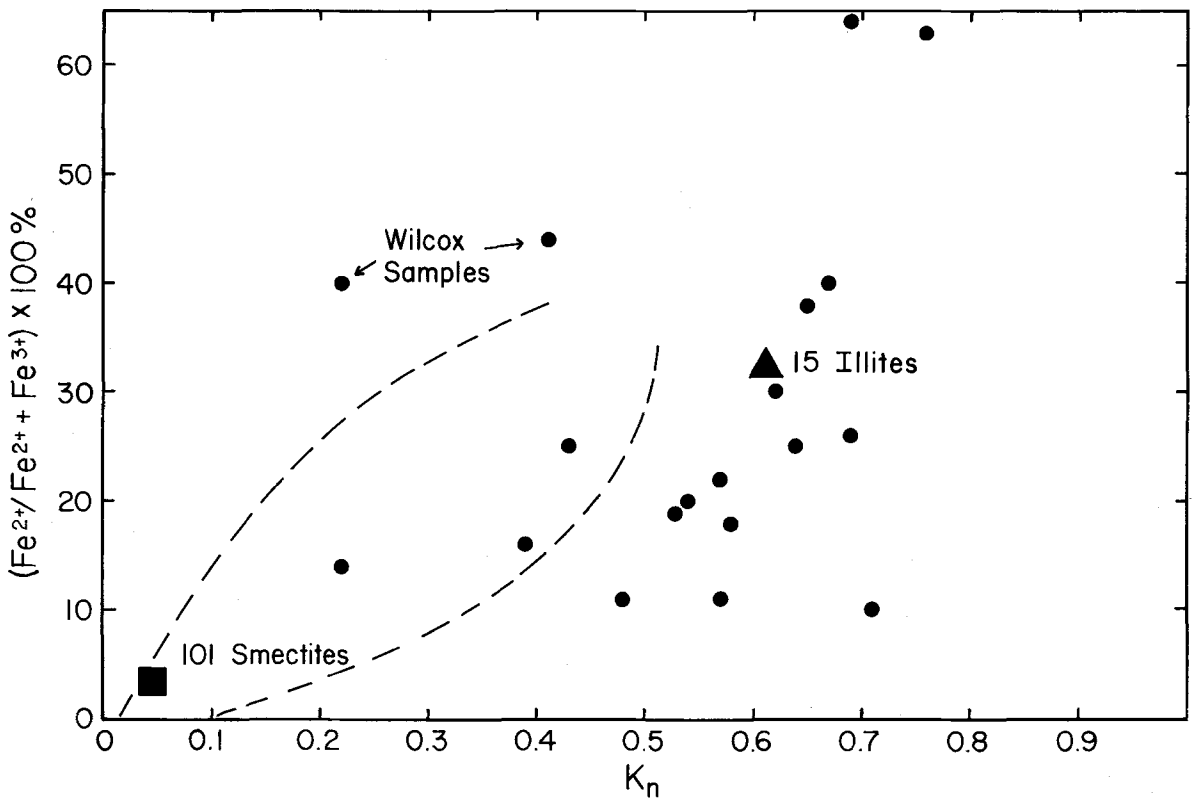

Figure 8. $Fe^{2+}/(Fe^{2+} + Fe^{3+}) \times 100\%$ vs. K_n in illites and I/S from shales and bentonites (Hower and Mowatt, 1966). Also shown are the averages of the same parameters of 101 smectites (montmorillonites and beidellites; Weaver and Pollard, 1973, p. 56) and 15 illites (Weaver and Pollard, 1973, p. 11). Samples reported on in this paper plot between the two dashed lines.

action for which the oxidation of trapped organic matter is the complementary half-reaction. The mineralogy of the I/S suggests that such a redox reaction would have begun at about 60°C.

6. Data from the literature indicate that illites and I/S with a high percentage of illite layers have higher Fe^{2+}/Fe^{3+} values than montmorillonites and beidellites with a low percentage of illite layers; this supports the idea that iron reduction is a general phenomenon that accompanies and contributes to the conversion of smectites to illites.

ACKNOWLEDGMENTS

This study was carried out under National Science Foundation Grant EAR75-15010 and a West Georgia College Faculty Research Grant. The work of Patrick Highsmith and Doyle Albers was done as senior undergraduate research projects. John Reed, Suzanne Ortiz, and Mike Bohn helped with the sample preparation and mineral identifications. David Brackett drafted the figures. Dennis Eberl, Graham Thompson, and Samuel Savin critically read the manuscript and offered suggestions for improvement.

REFERENCES

Bischoff, J. L. (1972) A ferroan nontronite from the Red Sea geothermal system: *Clays & Clay Minerals* **20,** 217–223.

Bowen, L. H., Weed, S. B., and Stevens, J. G. (1968) Mössbauer study of micas and their potassium-depleted products: *Amer. Mineral.* **54,** 72–84.

Dolcater, D. L., Syers, J. K., and Jackson, M. L. (1970) Titanium as free oxide and substituted forms in kaolinites and other soil minerals: *Clays & Clay Minerals* **18,** 71–79.

Dunoyer de Segonzac, G. (1965) Les argiles du Crétace supérieur dans le basin de Douala (Cameroun): Problèmes de diagenèse: *Bull. Serv. Carte Geol. Alsace Lorraine* **17,** 287–310.

Foscolas, A. E. and Kodama, H. (1974) Diagenesis of clay minerals from Lower Cretaceous shales of North Eastern British Columbia: *Clays & Clay Minerals* **22,** 319–336.

Goodman, B. A., Russell, J. D., Fraser, A. R., and Woodhams, F. W. D. (1976) A Mössbauer and i.r. spectroscopic study of the structure of nontronite: *Clays & Clay Minerals* **24,** 52–59.

Hoffman, J. and Hower, J. (1979) Clay mineral assemblages as low grade metamorphic geothermometers: application to the thrust faulted Disturbed Belt of Montana, U.S.A.: *Soc. Econ. Paleontol. Mineral. Spec. Publ. No.* **26,** 55–79.

Hoffman, J., Hower, J., and Aronson, J. (1976) Radiometric dating of time of thrusting in the Disturbed Belt of Montana: *Geology* **4,** 16–20.

Hower, J., Eslinger, E., Hower, M., and Perry, E. (1976) The

mechanism of burial diagenetic reactions in argillaceous sediments, 1. Mineralogical and chemical evidence: *Geol. Soc. Amer. Bull.* **87,** 725–737.

Hower, J. and Mowatt, T. C. (1966) The mineralogy of illites and mixed-layer illite/montmorillonites: *Amer. Mineral.* **51,** 825–854.

Jackson, M. L. (1956) *Soil Chemical Analysis—Advanced Course:* University of Wisconsin, College of Agriculture, Dep. of Soils, Madison, Wisconsin, 894 pp.

Malathi, N., Puri, S. P., and Saraswat, I. P. (1969) Mössbauer studies of iron in illite and montmorillonites: *J. Phys. Soc. Jpn.* **26,** 680–683.

Medlin, J. H., Suhr, N. N., and Bodkin, J. B. (1969) Atomic absorption analysis of silicates employing $LiBO_2$ fusion: *At. Absorpt. Newsl.* **8,** 25–29.

Mudge, M. R. (1970) Origin of the Disturbed Belt in northwestern Montana: *Geol. Soc. Amer. Bull.* **81,** 377–392.

Mudge, M. R. (1972a) Prequaternary rocks in the Sun River Canyon area, northwestern Montana: *U.S. Geol. Surv. Prof. Pap.* **663-A,** 142 pp.

Mudge, M. R. (1972b) Structural geology of the Sun River Canyon and adjacent areas, northwestern Montana: *U.S. Geol. Surv. Prof. Pap.* **663-B,** 51 pp.

Muffler, L. J. and White, D. E. (1969) Active metamorphism of upper Cenozoic sediments in the Salton Sea geothermal field and the Salton Trough, Southwestern California: *Geol. Soc. Amer. Bull.* **80,** 157–182.

Osthaus, B. B. (1954) Chemical determination of tetrahedral ions in nontronites and montmorillonites: *Clays & Clay Minerals,* Proc. 2nd Nat. Conf., Nat. Acad. Sci.-Nat. Research Council Publ. **327,** 407–416.

Oxburgh, E. R. and Turcotte, D. L. (1974) Thermal gradients and regional metamorphism in overthrust terrains with special reference to the eastern Alps: *Schweiz. Mineral. Petrogr. Mitt.* **54,** 641–662.

Perry, E. and Hower, J. (1970) Burial diagenesis in Gulf Coast pelitic sediments: *Clays & Clay Minerals* **18,** 165–177.

Reynolds, R. C., Jr. and Hower, J. (1970) The nature of interlaying in mixed-layer illite-montmorillonites: *Clays & Clay Minerals* **18,** 25–36.

Rozenson, I. and Heller-Kallai, L. (1976a) Reduction and oxidation of Fe^{3+} in dioctahedral smectites: 1. Reduction with hydrazine and dithionite: *Clays & Clay Minerals* **24,** 271–282.

Rozenson, I. and Heller-Kallai, L. (1976b) Reduction and oxidation of Fe^{3+} in dioctahedral smectites: 2. Reduction with sodium sulfide solutions: *Clays & Clay Minerals* **24,** 283–288.

Rozenson, I. and Heller-Kallai, L. (1976c) Mössbauer spectra of dioctahedral smectites: *Clays & Clay Minerals* **25,** 94–101.

Rozenson, I. and Heller-Kallai, L. (1978) Reduction and oxidation of Fe^{3+} in dioctahedral smectites: 3. Oxidation of octahedral iron in montmorillonites: *Clays & Clay Minerals* **26,** 88–92.

Shaw, D. M. (1956). Geochemistry of pelitic rocks. Part III. Major elements and general geochemistry: *Geol. Soc. Amer. Bull.* **67,** 919–934.

Taylor, G. L., Ruotsala, A. P., and Keeling, R. O., Jr. (1968) Analysis of iron in layer silicates by Mössbauer spectroscopy: *Clays & Clay Minerals* **16,** 381–391.

Weaver, C. E. (1960) Possible uses of clay minerals in the search for oil: *Amer. Assoc. Petrol. Geol. Bull.* **44,** 1505–1518.

Weaver, C. E. and Beck, K. C. (1971) Claywater diagenesis during burial: How mud becomes gneiss: *Geol. Soc. Amer. Spec. Pap.* **134,** 96 pp.

Weaver, C. E. and Pollard, L. D. (1973) *The Chemistry of Clay Minerals:* Elsevier-Holland, New York, 213 pp.

Weaver, C. E., Wampler, J. M., and Pecuil, T. E. (1967) Mössbauer analysis of iron in clay minerals: *Science* **156,** 504–508.

(Received 5 July 1978; accepted 23 April 1979)

Резюме—Бентониты мелового периода были собраны в обнажениях Свитграс Арк и Дистербд Белт в Монтане. Смешанно-слойные компоненты бентонитов иллит-смектит (И/С) из Свитграс Арк имеют 0 до 25% слоев иллита и в них не было обнаружено структурного Fe^{2+}, тогда как пробы из Дистербд Белт имеют примерно от 25 до 90% слоев иллита, и все содержат Fe^{2+}. Положительная корреляция (r = 0,89) существует между процентным содержанием структурного жедеза (Fe^{2+}) и количеством фиксированного межслоя K в И/С.

Большое процентное содержание слоев иллита в пробах из Дистербд Белт относится за счет реакций, присходящих при повышенных температурах, обусловленных залеганием бентонитов под надвиговыми пластами. Увеличение Fe^{2+}/Fe^{3+} с повышением процентного содержания слоев иллита, на основе опыта, связывается с окислительно-восстановительной реакцией, включающей окисление органического материала. Хотя при рассмотрении всех образцов не существует статистических доказательств увеличения октаэдрического заряда с увеличением содержания слоев иллита, восстановление железа могло обусловить от 10 до 30% увеличения общего структурного заряда, который возник в каждом образце в течение метаморфизма. Остающееся увеличение структурного заряда может быть отнесено за счет замещения Al^{3+} кремнием Si^{4+} в тетраэдрических слоях.

Resümee—Kreidehaltige Bentonite wurden in Zutageliegen vom "Sweetgrass Arch" und "Disturbed Belt" in Montana gesammelt. Die Illit-Smektit (I/S) Anteile der Wechselschicht der Bentonite vom "Sweetgrass Arch" haben von 0 bis 25% Illitschichten und kein feststellbares strukturelles Eisen^{2+}, wohingegen die Proben vom "Disturbed Belt" ungefähr von 25 bis 90% illitschichten haben und alle enthalten Eisen^{2+}. Eine positive Abhängigkeit (r = 0,89) besteht zwischen dem Prozentsatz des strukturellen Eisen, welches als Eisen^{2+} vorkommt und der Menge der gehärteten Zwischenschicht K im I/S.

Der höhere Prozentsatz von Illitschichten in den Proben vom "Disturbed Belt" wird Reaktionen zugeschrieben, die mit erhöhten Temperaturen verbunden sind, die durch Vergrabung unter Schubschichten erzeugt wurden. Die Zunahme in Eisen^{2+}/Eisen^{3+} mit zunehmendem Prozentsatz von Illitschichten wird versuchsweise einer Redoxreaktion zugeschrieben, in der Oxidation von organischem Material beteiligt ist. Wenn alle Proben zusammen berücksichtigt werden, gibt es keine statistischen Beweise für die Zunahme in oktaedrischer Ladung mit Zunahme in Illitschichten. Eisenreduktion könnte jedoch soviel wie 10 bis 30% zu der Zunahme in gesamtstruktureller Ladung, welche in jeder gegebenen Probe vorkommt, beitragen. Der Rest der strukturellen Ladungszunahme kann der Substitution von Si^{4+} mit Al^{3+} in den tetraedrischen Plätzen zugeschrieben werden.

Résumé—Des bentonites du Crétacé ont été collectionés d'un affleurement de Sweetgras Arch et du Disturbed Belt du Montana. Les constituants illite-smectite à couches mélangées (I/S) des bentonites de Sweetgras Arch ont de 0 à 25% de couches d'illite et pas de Fe^{2+} détectible, alors que les échantillons du Disturbed Belt ont de 25 à 90% de couches d'illite, et tous contiennent Fe^{2+}. Une corrélation positive (r = 0,89) existe entre le pourcentage de fer de composition qui est Fe^{2+} et la quantité de K fixe intercouche dans I/S.

Le pourcentage plus élevé des couches d'illite dans les échantillons du Disturbed Belt est attribué à des réactions liées à de hautes températures causées par l'enterrement sous des nappes de charriage. L'augmentation de Fe^{2+}/Fe^{3+} allant de pair avec l'augmentation des pourcentages des couches d'illite est tentativement attribué à une réaction rédox impliquant l'oxidation de matière organique. Bien qu'il n'y ait aucune évidence statistique d'une augmentation de charge octaèdrique accompagnant une augmentation dans les couches d'illite lorsque tous les échantillons sont considérés ensemble, la réduction de fer peut avoir contribué de 10 à 30% à l'augmentation de la charge totale de composition qui s'est passée pendant le métamorphisme de tout échantillon. Le reste de l'augmentation de charge de composition peut être attribué à la substitution d'Al^{3+} à Si^{4+} dans les sites tétraèdriques.